



**HAL**  
open science

# Theoretical Performance of Coherent and Incoherent Detection for Zero-Forcing Receive Antenna Shift Keying

Ali Mokh, Matthieu Crussière, Maryline Héland, Marco Di Renzo

► **To cite this version:**

Ali Mokh, Matthieu Crussière, Maryline Héland, Marco Di Renzo. Theoretical Performance of Coherent and Incoherent Detection for Zero-Forcing Receive Antenna Shift Keying. IEEE Access, 2018, 6, pp.39907-39916. 10.1109/ACCESS.2018.2851364. hal-01861300

**HAL Id: hal-01861300**

**<https://univ-rennes.hal.science/hal-01861300>**

Submitted on 10 Sep 2018

**HAL** is a multi-disciplinary open access archive for the deposit and dissemination of scientific research documents, whether they are published or not. The documents may come from teaching and research institutions in France or abroad, or from public or private research centers.

L'archive ouverte pluridisciplinaire **HAL**, est destinée au dépôt et à la diffusion de documents scientifiques de niveau recherche, publiés ou non, émanant des établissements d'enseignement et de recherche français ou étrangers, des laboratoires publics ou privés.

# Theoretical Performance of Coherent and Incoherent Detection for Zero-Forcing Receive Antenna Shift Keying

Ali Mokh<sup>[1]</sup>, Matthieu Crussière<sup>[1]</sup>, Maryline H elard<sup>[1]</sup>, and Marco Di Renzo<sup>[2]</sup>,  
[1] Univ Rennes, INSA Rennes, CNRS, IETR – UMR 6164, F-35000 Rennes, France  
[2] Laboratoire des Signaux et Syst emes, CNRS, CentraleSup elec, Univ Paris Sud,  
Universit  Paris-Saclay, 91192 Gif-sur-Yvette, France

**Abstract**—Receive Antenna Shift Keying (RASK) is a MIMO transmission scheme that has recently been under study, because of its low detection complexity and its ability to transmit spatial bits by targeting one of the receive antennas, whose index is used as spatial constellation to transmit a set of bits equal to base-two logarithm of the number of receive antennas. Zero-Forcing (ZF) precoding can be used at the transmitter side to steer the signal towards the targeted antenna. Different detection schemes can be implemented in order to detect the RASK information. Moreover, for the sake of low complexity and low power consumption, decreasing the number of RF chains by the use of switched antennas can also be implemented. In this paper, we lead a theoretical analysis of the transmission of spatial symbols in RASK, using the ZF precoding. Two detection schemes relying on maximum likelihood (ML) detection are presented and proved to be reduced to a simple Single-Tap detector. One, called coherent ML (CML), needs one RF chain per receive antenna and the other one, named incoherent ML (IML), is based on an envelop detector and needs only one RF chain for the entire antenna array. Closed-form expressions of the Bit Error Rate (BER) are derived for each scheme and validated through simulation. The CML detector is demonstrated to obviously outperform the IML detector in terms of BER but at the cost of higher complexity and power consumption. We then proposed to use switches to reduce the number of RF chains, thus trading off some performance against complexity. At some point, IML is shown to outperform CML, depending on the number of switches, RF chains, and system configuration. This turning point is analytically calculated and validated through simulations, and so can be used for further system comparison studies.

**Index Terms**—Spatial Modulation (SM), Receive Antenna Shift Keying (RASK), Beamforming, multiple input multiple output (MIMO).

## I. INTRODUCTION

Since the early 2000s, Spatial Modulation (SM) has established itself as a promising transmission concept for low complexity devices and low power consumption [1]. SM exploits the index of transmit or receive antennas to transmit additional information bits commonly referred to as spatial bits and spatial symbols [2]–[5]. The main distinguishable feature of SM–MIMOs is that they map additional information bits onto an “SM constellation diagram”, where each constellation element is constituted by either one or a subset of antenna elements [6].

The first proposed SM schemes concerned open loop systems, because they required no channel state information at the transmitter side (CSIT). They are called transmit SM (TSM) schemes and mainly relies on Space Shift Keying (SSK) strategies [7]: the spatial information is carried out by the index of the transmit antenna (TA) which should then be recognized by the receiver through proper signal analysis and assuming available CSI at the receiver (CSIR) [8], [9]. Hence, TSM takes advantage of the (assumed) unique propagation characteristics of each spatial link of the system [10] to build a bijective relationship between the active antennas and the spatial symbols. During the past decade, advanced TSM schemes have been developed in order to increase the spectral efficiency of conventional SSK, by expanding the number of active antennas. One can cite Generalized Spatial Modulation (GSM) [11], Generalized SSK (GSSK) [12], [13], and other enhanced schemes as in [14]–[16]. All these advanced schemes overcome the constraint considered in conventional SSK-based TSM systems that the number  $N_t$  of TAs has to be a power of two.

On one other hand, SM principles can be transposed at the receiver side, leading to the receive SM (RSM) concept. As introduced in [17], RSM can also be referred to as Transmitter Preprocessing Aided Spatial Modulation (TPSM), since it relies on a preprocessing or spatial pre-coding operation that exploits the channel state information at the transmitter (CSIT), so as to target one of the antennas of the receiver. Hence, in contrast to TSM, which uses the SSK concept to map the information bits to the TA indices, RSM carries out a kind of pre-SSK operation to map them to the indices of the receive antennas (RA).

As for the preprocessing operation, various options can be considered. Generally speaking, RSM schemes assume MIMO systems with more transmit than receive antennas to allow for favorable spatial preprocessing. One first solution introduced in [18] and further experimented and studied in [19][20], is referred to as receive antenna shift keying (RASK). In these papers, Time Reversal (TR) is used as precoding technique to concentrate the signal energy towards a targeted antenna. With RASK, a simple demodulation can be carried out based on the maximization of the real part of the received signal.

Since one single antenna is targeted at a time, efficiency is however limited to  $\log_2 N_r$ , with  $l$  of receive antennas. Another solution is to implement Zero Forcing (ZF) precoding at the transmitter in order to cancel the received signals at non targeted antennas. At the receiver, a maximum likelihood detector is used to estimate the signal at the targeted receive antenna [21]. As in traditional RSM schemes, enhanced RSM schemes have recently been developed in the downlink from one base station (BS) to multiple user devices to increase the spectral efficiency while maintaining low complexity [22]–[26].

In this paper, we propose to lead a theoretical analysis of the performance of the RASK scheme when it is considered as a preprocessing scheme, for a variety of detectors and depending on the number of antennas. Antennas are chosen to be used for complexity and power issues. We introduce two detection schemes: coherent and incoherent detection, both based on the maximum likelihood (ML) criterion. The coherent detector (CML) uses multiple RF chains as the number of receive antennas. The incoherent detector (IML) is only based on an envelope detector at the RF level. In each case, we demonstrate that the optimal receiver can be reduced to a single tap detector, which is favorable in terms of computational complexity. The performance analysis of the achievable Bit Error Rate (BER) is derived and compared through simulations. Then, in order to reduce the RF frond-end complexity of the coherent system, we proposed to decrease the number of RF chains by means of switches, as already proposed for TSM in [27]. The analytical study is then pursued to assess the performance degradation when reducing the number of RF links. Finally, a turning point in the performance is identified between the IML solution and the switched CML solution when the number of RF chains varies.

The rest of the paper is organized as follows. In Section II, the principle of RASK is restated, and we explain the transmission of a sequence of bits. In Section III, the system model and the block diagram of the RASK scheme are detailed. This is followed by the efficient implementation of an optimal receiver, and analytic study of the BER performance for both detection methods of RASK in Section IV. Simulation results and theory validations are also provided. In Section V, we proposed to reduce the complexity of coherent detector using switches, and the performance degradation is evaluated. Also, the equivalence point of two detection scheme is derived and evaluated. A conclusion is drawn in Section VI.

## II. RECEIVE ANTENNA SHIFT KEYING SYSTEM MODEL

### A. Principle of RASK

In this section, let us first give a brief reminder of the RASK concept. RASK applies SM at the receiver side by means of spatial focusing techniques [18]. More precisely, assuming a transmitter with  $N_T$  antennas and a receiver with  $N_R$  antennas, RASK consists in exploiting the transmit antenna array to form spatial beams and target one of the  $N_R$  receive antennas during each symbol duration. The index of the targeted antenna is

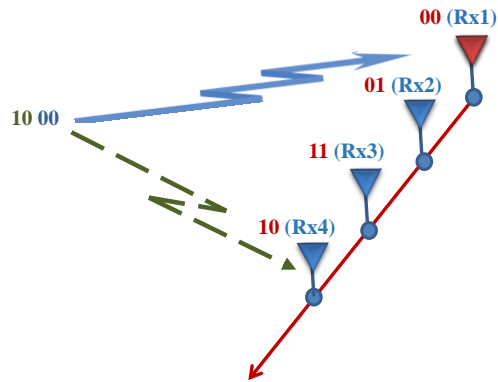


Figure 1. Example of RASK system with  $N_R = 4$

associated to a predefined set of information bits, meaning that information is transmitted according to a predefined bit-to-antenna mapping instead of a bit-to-complex-symbol mapping as used in classical digital communication schemes. As RASK considers one single targeted antenna at a time, the number  $m$  of bits conveyed by a RASK symbol is simply:

$$m = \log_2(N_R).$$

For a convenient RASK operation, the number of useful receive antenna should, therefore, be a power of two.

Figure 1 provides an illustrating example for a RASK scheme with  $N_R = 4$ , i.e. in which  $m = 2$  bit per symbol are transmitted. The corresponding spatial mapping table is given as follows:

Targeted antenna $R_i$	$R_1$	$R_2$	$R_3$	$R_4$
M-ary symbol	00	01	11	10

Figure 1 considers the transmission of a sequence of 4 bits, or equivalently of two consecutive spatial symbols. For this considered sequence and according to the above mapping, the focused antennas are  $R_1$  first, and  $R_4$  then.

As may be understood, the performance of RASK essentially relies on two main aspects which are on the one hand the capability of the transmitter to accurately focus the signal towards the desired antenna, and on the other hand the efficiency of the detection algorithm at the receiver side for proper decision about the targeted antennas. In the following parts, the detailed system model making use of the RASK scheme is presented, discussing the choice of the preprocessing and detection algorithms.

### B. System Model

The block diagram of a RASK transmission chain is depicted in Figure 2. According to the  $N_T \times N_R$  multiple-antenna system architecture previously considered, the RASK system can be modeled using the following matrix based input-output signal expression

$$\mathbf{Y} = f \cdot \mathbf{H} \underbrace{\mathbf{W} \mathbf{X}}_{\mathbf{S}_k} + \mathbf{N}, \quad (1)$$

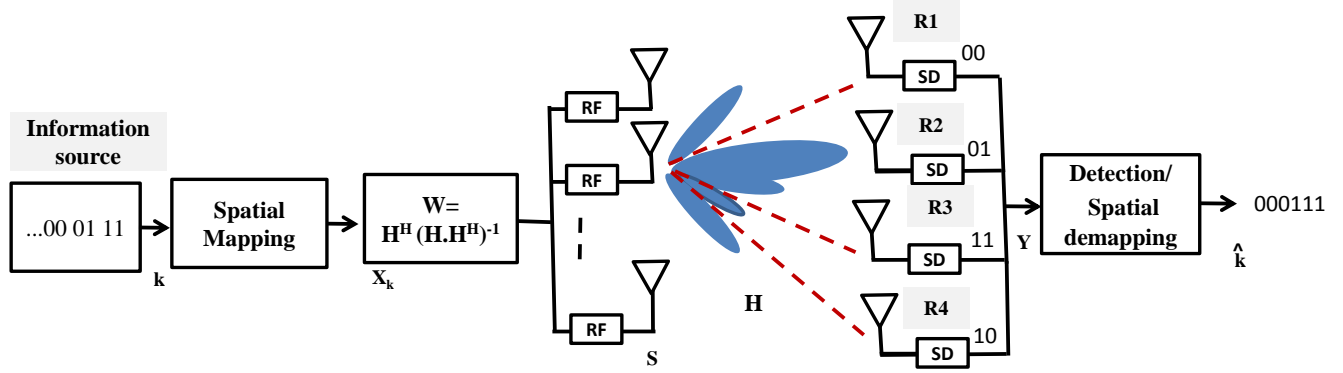


Figure 2. Block diagram of RASK

where  $\mathbf{H} \in \mathbb{C}^{N_R \times N_T}$  is the MIMO flat fading channel matrix with elements  $h_{j,i}$  representing the complex channel gain between the  $i$ th transmit antenna, denoted  $T_i$ , and the  $j$ th receive antenna, denoted  $R_j$ .  $\mathbf{S}_k \in \mathbb{R}^{N_T \times 1}$  is the vector of the complex samples sent through the  $N_T$  transmit antennas and intended to focus towards receive antenna  $R_k$ .  $\mathbf{Y} \in \mathbb{C}^{N_R \times 1}$  is the vector of the received signals on all receive antennas and  $\mathbf{N} \in \mathbb{C}^{N_R \times 1}$  is the vector of additive white Gaussian noise (AWGN) samples  $\eta_j$  such that  $\eta_j \sim \mathcal{CN}(0, \sigma_n^2)$ . Spatial focusing is obtained through the pre-processing step modeled by matrix  $\mathbf{W} \in \mathbb{C}^{N_T \times N_R}$  which transforms the vector of spatial symbols  $\mathbf{X}_k$  into the vector of transmitted samples  $\mathbf{S}_k$ . Finally,  $f$  is a normalization factor used to guarantee that the average total transmit power  $\bar{P}_t$  remains constant independently on the spatial symbol vector and the pre-processing matrix.

The spatial symbols  $\mathbf{X}_k$  result from the spatial mapping step. They are formed such that the entries  $x_k(j)$  of  $\mathbf{X}_k$  verify  $x_k(j) = A$  for  $j = k$  and  $x_k(j) = 0$ ,  $\forall j \neq k$ , where  $k$  is the index of the antenna that should be targeted according to the spatial mapping. In other words,  $\mathbf{X}_k$  can be written as

$$\mathbf{X}_k = \begin{bmatrix} 0 & \dots & \underbrace{A}_{k\text{th position}} & \dots & 0 \end{bmatrix}^T. \quad (2)$$

Note that average transmit power  $\bar{P}_t$  equals  $A^2$  in that case.

### C. Pre-processing

The transmitter uses the pre-processing step to create a beam that will concentrate a higher amount of energy towards the targeted receive antenna than towards the other antennas. The pre-processing block requires knowledge of the channel response at the transmitter. Focusing properties are related to the pre-processing scheme performed by the transmitter. It can be of signal-to-noise-ratio (SNR) maximization kind such as maximum ratio transmission (MRT), or of interference cancellation kind such as Zero-Forcing (ZF) beamforming. In this paper, the ZF technique is employed, where the pseudo-inverse of the channel matrix is used as a pre-filter:

$$\mathbf{W} = \mathbf{H}^H (\mathbf{H}\mathbf{H}^H)^{-1} \quad (3)$$

This technique allows a cancellation of the received energy on the non-targeted antennas. However, the required number of

antennas should satisfy the constraint  $N_R \leq N_T$  so that the matrix inversion remains possible.

The equation of transmitted signal is written as:

$$\mathbf{S} = f \times \mathbf{W}\mathbf{X} \quad (4)$$

Moreover,

$$f = \frac{1}{\sqrt{\mathbb{E}_k \{ \text{Tr}(\mathbf{X}_k^H \mathbf{W}^H \mathbf{W} \mathbf{X}_k) \}}} \quad (5)$$

where  $\text{Tr}(\cdot)$  holds for the trace of matrix and  $\mathbb{E}_k$  stands for the expectation over  $k$ . We have:

$$\text{Tr}(\mathbf{X}_k^H \mathbf{W}^H \mathbf{W} \mathbf{X}_k) = A^2 \sum_i \|w_{i,k}\|^2. \quad (6)$$

$\mathbf{X}$  takes  $N_R$  different signatures depending on the index of the targeted antenna, so the expectation is applied to  $k$ :

$$\mathbb{E}_k \{ \text{Tr}(\mathbf{X}_k^H \mathbf{W}^H \mathbf{W} \mathbf{X}_k) \} = \frac{A^2}{N_R} \text{Tr}(\mathbf{W}^H \mathbf{W}) \quad (7)$$

Finally, Eq. (5) becomes :

$$f = \sqrt{\frac{N_R}{A^2 \text{Tr}(\mathbf{W}^H \mathbf{W})}} \quad (8)$$

### D. Receiver Block Diagram

The RASK receiver has to detect the targeted antenna between the  $N_R$  receive antennas in order to estimate the spatial symbol. Various detection algorithms can be used for the estimation of the targeted antenna depending on the complexity which can be afforded by the receiver [18]. Using the expression of the receive signal vector in Eq. (1) detected by a Signal Detector "SD", and the expression of the preprocessing matrix in Eq. (3), it is then straightforward to obtain:

$$\mathbf{Y} = f \times \mathbf{X} + \mathbf{N} \quad (9)$$

At the level of the received antenna  $R_j$ , the received signal then simply writes:

$$y_j = f \times x_j + \eta_j. \quad (10)$$

Two schemes of receiver are proposed, where coherent and incoherent detections are used and studied:

- Coherent Maximum Likelihood detector (CML), based on the application of the maximum likelihood criterion, coherent to the complex received signal.
- Incoherent Maximum Likelihood detector (IML), a non coherent detector that applies the ML criterion to the received power.

### III. DETECTION SCHEMES

In this section, different detection schemes and algorithms are presented, and a closed form of the BER conditioned by the channel, i.e. for a given channel realization, is calculated.

#### A. Coherent Maximum Likelihood (CML)

From Eq. (10), a given detector has to analyze the following set of signals:

$$\forall j, \quad y_j = \begin{cases} f \times A + \eta_j & \text{if } R_j \text{ is the targeted antenna} \\ \eta_j & \text{otherwise} \end{cases} \quad (11)$$

Since the ZF precoding scheme is used, no interference appears between receive antennas. The maximum likelihood receiver has been presented and studied in [22], where the equation of this detector is:

$$\hat{k} = \text{Arg min}_j \left\{ \|\mathbf{Y} - f\mathbf{X}_j\|^2 \right\} \quad (12)$$

The CML detector saves the signatures of all possible spatial symbols transmitted ( $N_R$  signatures) in a stage of calibration, and choose, at each time symbol, the one that is closer to the received signal in the Euclidean distance. Referring to the same study, the Pairwise Error Probability (PEP) of the CML detector for the spatial modulation is:

$$\text{PEP} = Q(f \times A / \sigma_n). \quad (13)$$

where  $Q(\cdot)$  denotes the normal cumulative distribution function.

#### B. Efficient Implementation of the ML detector

**Theorem 1.** *In RASK system with only spatial symbol transmission, if ZF preprocessing is employed, the optimal detector is reduced to a Single Tap Maximum real part comparator.*

*Proof.* Using ZF pre-processing, the received signal at the targeted antenna will exhibit the same phase than that of the emitted signal due to the phase compensation effect. Reconsidering the derivations of PEP in [22], in order to simplify the detection algorithm of ML, supposing that  $\mathbf{X}_k$  is the transmitted spatial symbol:

$$\begin{aligned} \text{PEP} &= \mathcal{P} \left( \|\mathbf{Y} - f\mathbf{X}_k\|^2 > \|\mathbf{Y} - f\mathbf{X}_j\|^2 \right) \\ &= \mathcal{P} \left( \sum_{i=1}^{N_R} \|\eta_i\|^2 > \sum_{i=1}^{N_R} \|\eta_i\|^2 + 2(fA)^2 \right. \\ &\quad \left. + 2fA \times \Re\{\eta_k - \eta_j\} \right) \\ &= \mathcal{P} \left( \Re\{\eta_j\} > fA + \Re\{\eta_k\} \right) \end{aligned} \quad (14)$$

So in such receiver, if the transmitted signal is real, a valid detection is maintained if the targeted antenna detects the maximum value of real amplitude part, and the same performance could be obtained with a simpler detection algorithm.  $\square$

Considering that the phase of targeted signal  $s_j = A, \phi_A$ , is known at the receiver, the receiver can compensate it and choose the antenna index that has the maximum real part. So we have:

$$\hat{k} = \text{Arg max}_j \Re\{y_j^0\} \quad (15)$$

where

$$y_i^0 = y_i \times e^{-\phi_A} \quad (16)$$

And this decoder could also be described as:

$$\forall j \in [1; N_R], \Re\{y_j^0\} \leq \Re\{y_k^0\} \quad (17)$$

This algorithm avoids the receiver to carry out the channel estimation step, and thus reduces the computational complexity of the receiver. Note that for a complex CML detector in another scenario,  $4N_R^2$  multiplications and  $5N_R^2$  additions/subtractions are needed, while the reduced CML for ZF precoded RASK is a Single-Tap detector using  $N_R - 1$  comparators. Otherwise, in case of interference, as if we use another preprocessing technique, the reduced CML described above is no more equivalent to the true CML.

#### C. Closed Form of BER with CML detector

**Theorem 2.** *The closed form of BER obtained with a coherent ML receiver conditioned by the channel  $\mathbf{H}$  for a ZF RASK scheme is given by the equation:*

$$\begin{aligned} \mathcal{P}_e &= \frac{N_R}{2 \cdot (N_R - 1)} \int_{-\infty}^{+\infty} \frac{1}{\sqrt{\pi\sigma_n^2}} e^{-\frac{(t-fA)^2}{\sigma_n^2}} \\ &\quad \times \left[ 1 - Q\left(\frac{t\sqrt{2}}{\sigma_n}\right) \right]^{N_R-1} dt. \end{aligned} \quad (18)$$

*Proof.* The formula that derives the analytic Average BER  $\mathcal{P}_e$  for RASK scheme is:

$$\mathcal{P}_e = \frac{1}{m} \cdot \mathbb{E} \left\{ \sum_k \sum_{j \neq i}^{N_R} \mathcal{P}(\mathbf{X}_k \rightarrow \mathbf{X}_j) \times d(\mathbf{X}_k, \mathbf{X}_j) \right\}. \quad (19)$$

where  $d(\mathbf{X}_k, \mathbf{X}_j)$  is the Hamming distance between two spatial symbols  $\mathbf{X}_k$  and  $\mathbf{X}_j$ . It is shown that the received real amplitude over all non-targeted antennas follows the same probability distribution, i.e.  $\mathcal{N}(0, \sigma_n^2/2)$ , so that the Eq. (19) can be expressed as:

$$\begin{aligned} \mathcal{P}_e &= \frac{1}{m} \mathbb{E} \left\{ \sum_k \sum_{j \neq i}^{N_R} d(\mathbf{X}_k, \mathbf{X}_j) \right\} \mathcal{P}(\mathbf{X}_k \rightarrow \mathbf{X}_{j, j \neq k}) \\ &= \frac{1}{\log_2(N_R)} \frac{N_R \log_2(N_R)}{2(N_R - 1)} \mathcal{P}(\mathbf{X}_k \rightarrow \mathbf{X}_j, j \neq k) \\ &= \frac{N_R}{2 \cdot (N_R - 1)} \mathcal{P}(\mathbf{X}_k \rightarrow \mathbf{X}_j, j \neq k) \end{aligned} \quad (20)$$

where  $\mathcal{P}(\mathbf{X}_k \rightarrow \mathbf{X}_j, j \neq k)$  is the Symbol Error Rate (SER). Another way to resolve this equation consist in evaluating the complementary of the SER, i.e.:

$$\mathcal{P}(\mathbf{X}_k \rightarrow \mathbf{X}_j, j \neq k) = 1 - \mathcal{P}[\Re\{y_{j,j \in [1:N_R]}\} < \Re\{y_k\}] \quad (21)$$

where

$$\Re\{y_i\} \sim \mathcal{N}(f, \sigma_n^2/2). \quad (22)$$

Moreover, from appendix A, the left-hand side of the equation above can be presented by the integral:

$$\mathcal{P}[\Re\{y_{j,j \in [1:N_R]}\} < \Re\{y_k\}] = \int_{-\infty}^{+\infty} f_{y_k}(t) \prod_{j=1, j \neq k}^{N_R} F_{y_j}(t) dt \quad (23)$$

where  $f_{y_k}(t)$  is the probability density function of  $y_k$ :

$$f_{y_k}(t) = \frac{1}{\sqrt{\pi\sigma_b^2}} e^{-\frac{(t-fA)^2}{\sigma_n^2}},$$

and  $F_{y_j}(t)$  is the cumulative density function of  $y_j$ :

$$F_{y_j}(t) = 1 - Q\left(\frac{t\sqrt{2}}{\sigma_n}\right).$$

So we have:

$$\begin{aligned} & \mathcal{P}[\Re\{y_{j,j \in [1:N_R]}\} < \Re\{y_k\}] \\ &= \int_{-\infty}^{+\infty} \frac{1}{\sqrt{\pi\sigma_n^2}} e^{-\frac{(t-fA)^2}{\sigma_n^2}} \prod_{j=1, j \neq k}^{N_R} F_{y_j}(t) dt \\ &= \int_{-\infty}^{+\infty} \frac{1}{\sqrt{\pi\sigma_n^2}} e^{-\frac{(t-fA)^2}{\sigma_n^2}} \left[ \prod_{j=1, j \neq k}^{N_R} \left(1 - Q\left(\frac{t\sqrt{2}}{\sigma_n}\right)\right) \right] dt \end{aligned}$$

**Lemma 3.** The BER for the CML can be approximated by:

$$\mathcal{P}_e \approx \frac{N_R}{2} Q\left(\frac{fA}{\sigma_n}\right)$$

*Proof.* For high Signal to Noise the value of  $\frac{1}{2} \operatorname{erfc}\left(\frac{t}{\sigma_n}\right)$  becom (24) could be approximated by:

$$\begin{aligned} & \mathcal{P}(\Re\{y_{j,j \in [1:N_R]}\} < \Re\{y_k\}) \\ & \approx \int_{-\infty}^{+\infty} \frac{1}{\sqrt{\pi\sigma_n^2}} e^{-\frac{(t-fA)^2}{\sigma_n^2}} \left[ \prod_{j=1, j \neq k}^{N_R} \left(1 - Q\left(\frac{t\sqrt{2}}{\sigma_n}\right)\right) \right] dt \\ & = \left[ 1 - (N_R - 1)Q\left(\frac{fA}{\sigma_n}\right) \right] \end{aligned}$$

And then the Eq. (20) becomes:

$$\begin{aligned} \mathcal{P}_e & \approx \frac{N_R}{2(N_R - 1)} \left[ 1 - \left( 1 - (N_R - 1)Q\left(\frac{fA}{\sigma_n}\right) \right) \right] \\ & = \frac{N_R}{2} Q\left(\frac{fA}{\sigma_n}\right). \end{aligned} \quad (27)$$

#### D. Incoherent Detection (IML)

The CML detector studied above need carrier and phase synchronization at the receiver side. Considering now the case of incoherent receiver that detects the received power at the antenna, without considering the phase of the signal. Fig. 3 shows the block diagram of an envelop detector that could be used for the detection without the need of RF block. A Pass-Band filter is first used to take only the carried signal centered by the transmission carrier frequency; followed by a power converter that converts the detected power into current. A low noise amplifier is also used to increase the overall SNR, before an integrator used to take the average mean detected power during the time symbol. In this case, the detector has to analyze the square of the norm of the complex received signals:

$$\forall j, \quad \|y_j\|^2 = \begin{cases} \|f \times A + \eta_j\|^2 & \text{if } R_j \text{ is the targeted antenna} \\ \|\eta_j\|^2 & \text{otherwise} \end{cases} \quad (28)$$

The receiver here estimate the spatial symbol by choosing the

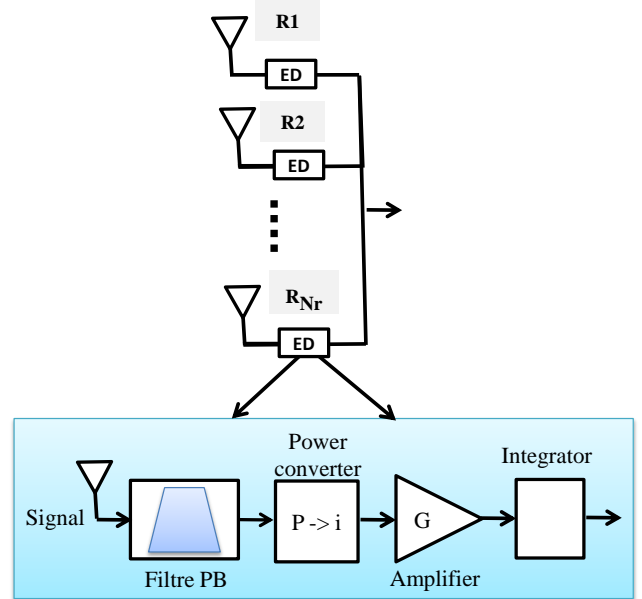


Figure 3. IML receiver with envelop detector

index of antenna that receives the maximum amount of power:

$$\hat{k} = \operatorname{Arg} \max_j \|y_j\|^2 \quad (29)$$

also described as:

$$\forall j \in [1; N_R], \|y_j\|^2 \leq \|y_{\hat{k}}\|^2 \quad (30)$$

**Theorem 4.** The closed form of BER of an IML detector conditioned by the channel  $\mathbf{H}$  for ZF RASK scheme is given

□

by the equation:

$$\mathcal{P}_e = \frac{N_R}{2 \cdot (N_r - 1)} \left[ 1 - \int_0^{+\infty} \frac{1}{\sqrt{2\pi}} \left( e^{-\frac{(x-m)^2}{2}} + e^{-\frac{(x+m)^2}{2}} \right) \times (1 - e^{-\frac{x^2}{2}})^{N_R-1} dx \right] \quad (31)$$

*Proof.* As we did for the performance analysis for the ML receiver in Eq. (20), the equation of the BER for this detector is:

$$\mathcal{P}_e = \frac{N_R}{2 \cdot (N_r - 1)} \cdot \left[ 1 - \mathcal{P} \left( \|y_{j,j \in [1:N_R]}\|^2 < \|y_k\|^2 \right) \right] \quad (32)$$

Moreover, we have:

$$\begin{aligned} \mathcal{P} \left( \|y_{j,j \in [1:N_R]}\|^2 < \|y_k\|^2 \right) &= \mathcal{P} \left( \|\eta_{j,j \neq i}\|^2 < \|f \cdot A + \eta_i\|^2 \right) \\ &= \mathcal{P} \left( |\eta'_{j,j \neq i}| < \left| \frac{\sqrt{2} \cdot f \cdot A}{\sigma_n} + \eta'_i \right| \right) \end{aligned} \quad (33)$$

where:

- $\left| \frac{\sqrt{2} \cdot f \cdot A}{\sigma_n} + \eta'_i \right| = |m + \eta'_i| = |\mathcal{J}|$  follows a Folded-Normal distribution, i.e.  $\mathcal{J} \sim \mathcal{N}(m, 1)$
- $|\eta'_j| = X \sim \mathcal{X}_2$  (Chi distribution)  $\forall j \in [1 : N_R], j \neq i$

so:

$$\begin{aligned} \mathcal{P} \left( \|y_{j,j \in [1:N_R]}\|^2 < \|y_k\|^2 \right) &= \mathcal{P}(X < |\mathcal{J}|) \\ &= \end{aligned} \quad (34)$$

for  $x < 0$ ,  $F_X(x) = 0$ , otherwise:

$$F_X(x) = P(1, x^2/2) = \frac{\gamma(1, x^2/2)}{\Gamma(1)} = 1 - e^{-\frac{x^2}{2}} \quad (35)$$

And the PDF of  $|\mathcal{J}|$  is:

$$f_{|\mathcal{J}|}(x) = \frac{1}{\sqrt{2\pi}} \left( e^{-\frac{(x-m)^2}{2}} + e^{-\frac{(x+m)^2}{2}} \right) \quad (36)$$

then the Eq. (33) becomes:

$$\begin{aligned} \mathcal{P} \left( \|y_{j,j \in [1:N_r]}\|^2 < \|y_k\|^2 \right) &= \\ \int_0^{+\infty} \frac{1}{\sqrt{2\pi}} \left( e^{-\frac{(x-m)^2}{2}} + e^{-\frac{(x+m)^2}{2}} \right) \cdot (1 - e^{-\frac{x^2}{2}})^{N_R-1} dx \end{aligned} \quad (37)$$

□

**Lemma 5.** *The BER for the IML receiver in ZF RASK scheme can be approximated by:*

$$\mathcal{P}_e \approx \frac{N_R}{4} e^{-(f \cdot A)^2 / 2\sigma_n^2} \quad (38)$$

*Proof.* For high SNR on the receiver, the value of  $e^{-\frac{x^2}{2}}$  become very small, and then the Eq. (37) can be approximated by:

$$\mathcal{P} \approx \int_0^{+\infty} \frac{1}{\sqrt{2\pi}} \left( e^{-\frac{(x-m)^2}{2}} + e^{-\frac{(x+m)^2}{2}} \right) \cdot (1 - (N_R - 1)e^{-\frac{x^2}{2}}) dx \quad (39)$$

After some mathematical manipulations, we obtain:

$$\mathcal{P} = 1 - \frac{N_R - 1}{2} e^{-\frac{(f \cdot A)^2}{2\sigma_n^2}}. \quad (40)$$

And so the Eq. (32) becomes:

$$\mathcal{P}_e \approx \frac{N_R}{4} \exp \left( -\frac{(f \cdot A)^2}{2\sigma_n^2} \right) \quad (41)$$

□

## E. Simulation Results

The performance of ZF-RASK system using different types of receivers is evaluated through the measurement of the BER versus the ratio between the symbol energies and noise spectral density, i.e.  $\frac{E_s}{N_0}$ . It is assumed that  $\mathbf{H}$  is a MIMO flat fading channel matrix where  $H_{j,i}$  are complex coefficients following i.i.d. Rayleigh distribution. The power for each sub-channel is normalized:

$$E[\|H_{j,i}\|^2] = 1 \quad (42)$$

Finally, we consider that the channel response is perfectly known at the transmitter, so that perfect ZF precoding is performed. Simulations are run by implementing a sufficient number of iterations for different channel realizations, and taking the mean value of the BER for each value of  $\frac{E_s}{N_0}$ .

Figure 4 gives the performance of RASK with  $N_T = 16$ , and  $N_R = 4$  and 8, using the CML (blue curves), respectively IML detectors (black curves). The performance based on simulations and the analytic study for each detection method are compared. As evident from the obtained curves, for high relative SNR, where the BER becomes less than  $10^{-1}$ , theoretical results perfectly match simulation results. Let us remind that increasing  $N_r$  directly translates into an increase of the spectral efficiency since the order  $M = 2^m$  of the SM is such that  $m = \log_2 N_R$  with RASK. It is also observed that increase in the order of the spatial modulation, leads to a degradation of the performance. Indeed, as  $N_R$  increases, the ZF pre-processing technique has to deal with a higher number of antennas on which interference has to be canceled. Also from the figure, it seems that the CML outperforms the incoherent one, which can be obviously concluded from the theoretical results.

## IV. REDUCING THE COMPLEXITY

### A. Influence of the number of RF chains

One of the main advantages of the SM at the transmitter was the possible reduction of the number of RF chain, to reduce the overall power. For receive SM, all receive antenna should listen to the received signal during time symbol, and so the reduction of the number of RF chains using switches (or analog multiplexer) lead to a degradation in the effective SNR. Let  $N_{RF}$  be the number of the RF chain at the receiver, and  $N_S$  the number of switches. In a fair scenario, each switch is connected to the same number of receive antennas and  $N_{RF} = N_S$  where each chain is connected to a switcher as shown in Figure 5. We are supposing that all switches are identical, let  $\tau$  be the delay of switching to change the state



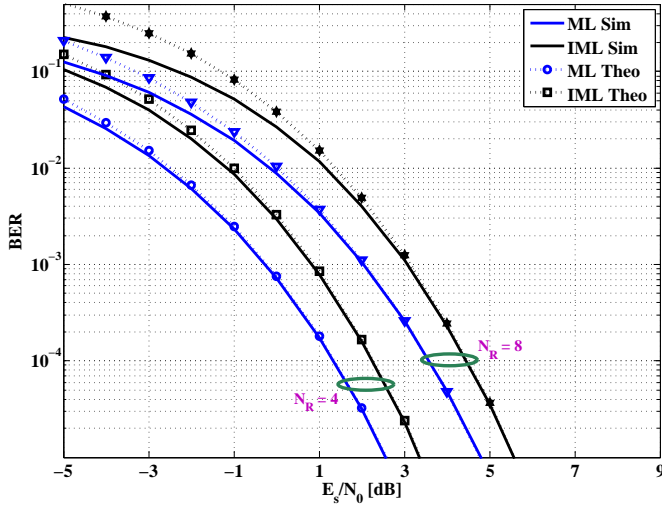


Figure 4. BER performance of  $16 \times 4$  and  $16 \times 8$  ZF RASK system using CML and IML detector over Rayleigh channel, simulation and theoretical results

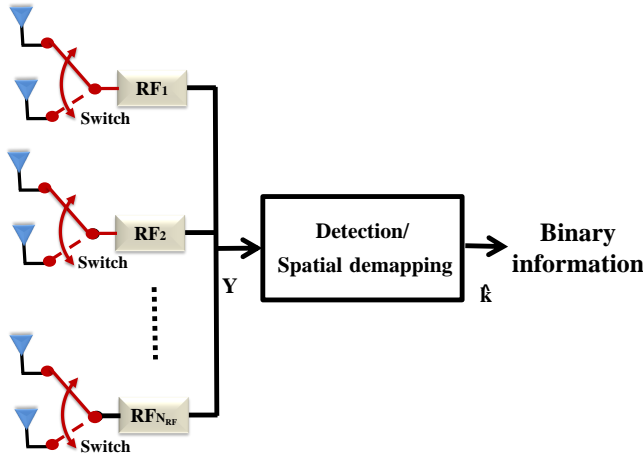


Figure 5. Receiver with  $N_{RF}$  RF chain and switch

of a switch port. Let  $\bar{P}_e$  be the mean total transmitted power per time symbol. The factor  $f$  at the transmitter normalizes the average transmit power to  $\bar{P}_e = A^2$ , and  $P_b = \sigma_n^2 = N_0 B$  is the noise power. Let  $\bar{P}_r$  be the mean of the received power at the targeted receive antenna. We have:

$$\bar{P}_r = \mathbb{E}_X\{\text{Tr}(\mathbf{S}_k^H \mathbf{H}^H \mathbf{H} \mathbf{S})\} = f^2 \times \bar{P}_e = f^2 \times A^2 = f^2 \times E_s \quad (43)$$

where  $E_s$  is the symbol energy. Supposing that the used band is  $B = D_s$ , where  $D_s$  is symbol rate, we have:

$$\text{SNR} = \frac{\bar{P}_r}{\sigma_n^2} = \frac{f^2 E_s D_s}{N_0 B} = \frac{f^2 E_s}{N_0} \quad (44)$$

The average time of listening over each receive antenna is  $T_l = T_s N_{RF} / N_R$ . Let  $\rho = \tau / T_l$ , and supposing that the waveform of the received signal is rectangular, the detected energy at the

received antenna  $E_d$  is equal to:

$$E_d = (1 - \rho) \bar{P}_r T_l = (1 - \rho) E_s N_{RF} / N_R \quad (45)$$

And we define ESNR as the efficient SNR resulted from the detected signal. we have then:

$$\text{ESNR} = (1 - \rho) \frac{f^2 E_s N_{RF}}{N_0 N_R} \quad (46)$$

For comparison purpose, we will consider the case of ideal switches, where  $\rho = 0$ . In the Figure 6, a ZF RASK scheme

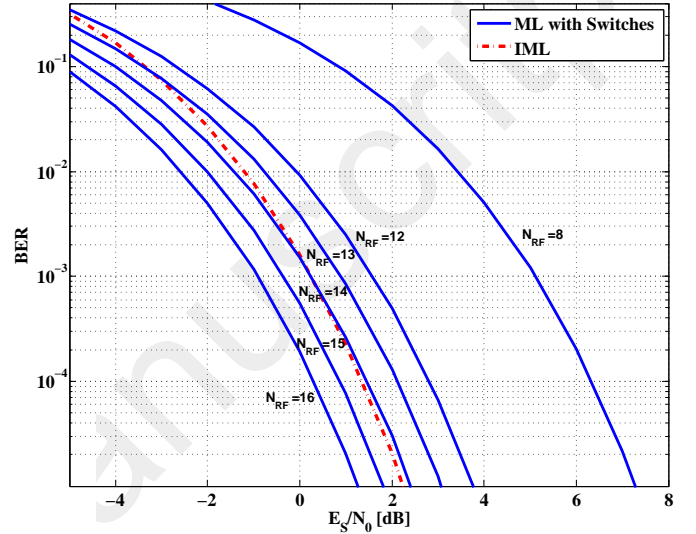


Figure 6. BER of  $32 \times 16$  ZF RASK using IML, or CML detection with variable number of RF chains using switches

with  $N_T = 32$  and  $N_R = 16$  configuration is considered. The BER performance using the IML is drawn, as well as the BER using the CML with different numbers of RF chains and ideal switches. As evident, decreasing the number of RF chains leads to BER degradation, and for a specific number of RF chain, the IML outperforms the CML at a predefined BER. For example, for a BER less than  $5 \times 10^{-4}$ , the IML outperforms the CML for  $N_{RF} \leq 14$ , and for a BER more than  $10^{-3}$  the IML performance occurs between the CML for  $N_{RF} = 13$  and  $N_{RF} = 14$ .

### B. Equivalence between Switched CML and IML

The system performance and the receiver complexity are two parameters to choose the better receiver. As shown before, reducing the number of RF chains to reduce the complexity or the power consumption, decrease the performance of the system, and at some point, the incoherent detector outperforms the coherent one. In order to fairly compare them, we can analytically calculate the equivalence of the two detection schemes. For a predefined system configuration, i.e.  $N_T$  and  $N_R$ , and predefined targeted BER, we are calculating the ratio  $\alpha = (1 - \rho) \frac{N_{RF}}{N_R}$  for a coherent system to achieve the BER with the same  $\text{SNR} = \left(\frac{fA}{\sigma_n}\right)^2$ . From Eq. (27), respectively



Eq. (41), the SNR needed to achieve certain BER, using the CML detector ( $\text{SNR}_{CML}$ ), respectively using IML detector ( $\text{SNR}_{IML}$ ) is:

$$\text{SNR}_{CML} = \frac{1}{\alpha} \left[ Q^{-1} \left( \frac{4}{N_R} \text{BER} \right) \right]^2, \quad (47)$$

which is independent on  $\alpha$ , respectively:

$$\text{SNR}_{IML} = -2 \times \ln \left( \frac{4}{N_R} \text{BER} \right). \quad (48)$$

**Proposition 1.** The equivalence point  $\alpha_E$  between CML and IML receiver is given by:

$$\alpha_E = - \frac{\left[ Q^{-1} \left( \frac{4}{N_R} \text{BER} \right) \right]^2}{\ln \left( \frac{4}{N_R} \text{BER} \right)}. \quad (49)$$

It could be proven by simple mathematical derivations of Eq.(47) and Eq.(48). Note that  $\alpha_E$  is independent on  $N_T$ , so the choice of the optimal receiver only depends on the receiver configuration and on the targeted BER.

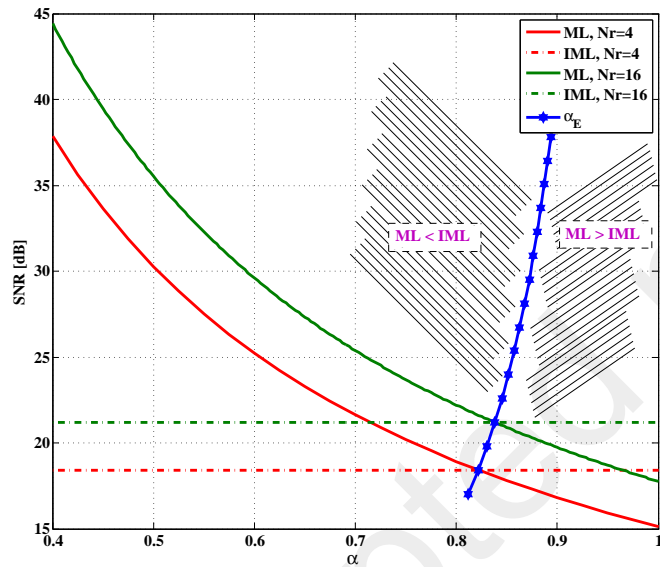


Figure 7. The needed SNR to achieve a  $\text{BER}=10^{-4}$  in a ZF RASK system with  $N_R = 4$  and  $N_R = 16$  using CML and IML detection, in terms of  $\alpha$

In Figure (7), the targeted BER is fixed at  $10^{-4}$ , and the needed SNR to achieve this BER is evaluated in function of  $\alpha$ , i.e. the number of RF chains, for  $N_R = 4$  and  $N_R = 16$ . Since the IML detection is independent on the number of RF chains (no RF chains needed), the value of  $\text{SNR}_{IML}$  is constant for each system configuration. Moreover,  $\text{SNR}_{CML}$  decreases when the number of RF chains increases, and at  $\alpha_E$  the two curves, for CML and IML, are crisscrossing. From Eq. (49), the analytical values for  $\alpha_E$  are 0.8217 for  $N_R = 4$ , and 0.8382 for  $N_R = 16$ , which can be validated by the curves. The blue curve gives the set of  $\alpha_E$  for different  $N_R$ . In the left side of the blue curve, the IML detector outperforms the CML detector with switches, and in the right side, the CML outperforms the IML. From  $\alpha_E$ , we

can deduce that the IML is a better choice when  $\alpha < \alpha_E$  in performance, in terms of complexity as well as power consumption. Asymptotically, the limit of Eq.(49) is equal to

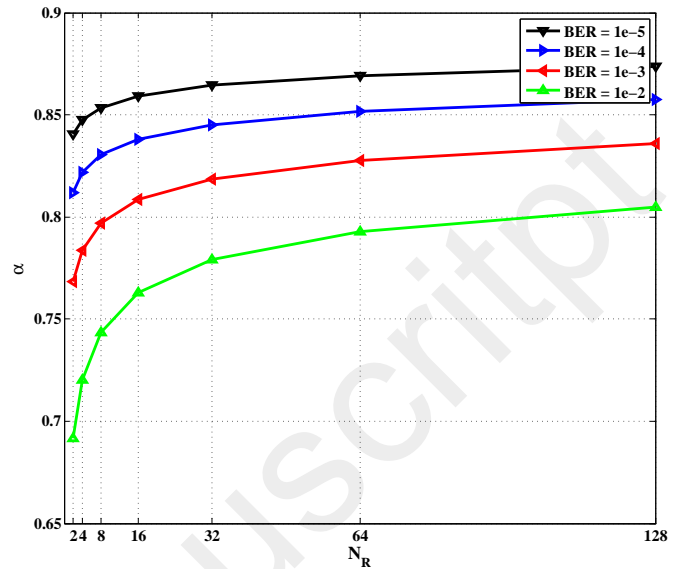


Figure 8. Variation of  $\alpha_E$  in terms of  $N_R$  for ZF RASK for different targeted BER.

1, since  $Q(x)$  could be approximated by  $e^{-x^2}$ , and so  $Q^{-1}(x)$  by  $-\ln(x)^2$ . The Fig. (8) shows the variation of  $\alpha_E$  in terms of  $N_R$  for different targeted BER. It is shown that  $\alpha_E$  increases when  $N_R$  increases and approaches to 1, and this means that for higher  $N_R$ , the performance of IML detector tends to be close to the CML detector even without switching (full of RF chains). Moreover, depending on the system and the channel coding used, for a targeted BER and for a specific system configuration, the IML outperforms the CML under certain  $N_{RF}$  also with lower complexity and cost. Then the CML will only be a better choice if  $N_{RF}$  is more or equal to  $\lceil \alpha_E \times N_R \rceil$ , where  $\lceil \cdot \rceil$  is the ceil operator.

Since  $\alpha$  takes real and continuous values, it is required to calculate the minimum number of RF chains to outperform the IML detector, which depends on  $\alpha_E$  and the switching time factor  $\rho$  :

$$\frac{N_{RF}}{N_R} = \left\lceil \frac{\alpha_E}{1 - \rho} \right\rceil. \quad (50)$$

Figure 9 shows the ratio of the number of RF chains for each receiver configuration,  $N_{RF}/N_R$ , needed to outperform the IML in terms of  $N_R$ , and for different values of  $\rho$ . It is shown that for  $\rho = 0$ , the ratio is higher than  $\alpha_E$  because of the discretization. Thus, the higher the switching factor, the higher the number of RF chains needed to increase the ESNR. Also, for  $\rho = 0.15$ , no RF reduction for  $N_R \leq 16$ , and so the switching there is no more effective.

## V. CONCLUSION

In this paper, we led a theoretical performance study on the RASK scheme using ZF preprocessing. Coherent and

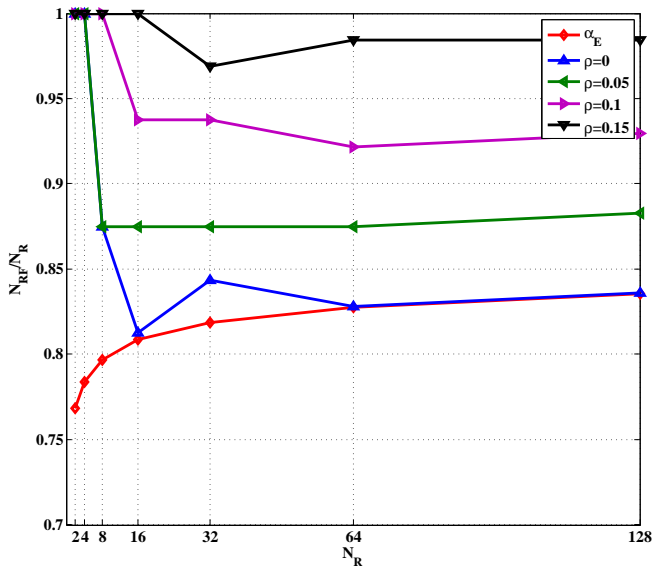


Figure 9. Ratio of number of RF chains for each receiver configuration of  $N_R$  for ZF RASK for different switching coefficient.

incoherent detection schemes using ML based detectors were studied, and we showed that such detectors could be reduced to simple Single-Tap detectors. The CML solution needs one RF chain per each receive antenna, whereas the IML scheme is based on simple envelop detectors. Our first contributions were at the level of the closed form expressions of the Bit Error Rate (BER) derived for each scheme, and validated through simulations. CML was shown to obviously outperform IML, but at the cost of higher complexity and higher power consumption. As a second contribution, we then proposed to reduce the number of RF chains in the CML solution by means of switches and provided the system analytical performance expression. We highlighted that the IML outperforms the ML depending on the number of switches and RF chains and on system configuration. This drove us to identify and analytically establish the turning point in the performance of the switched CML system compared to IML. From our analysis, we conclude that the incoherent detector could be a very good choice with lower complexity and power consumption.

#### APPENDIX A COMPARISON OF N RANDOM VARIABLES

Let  $X_1, X_2, \dots, X_n$  be  $n$  random variables, where each  $X_i$  follows a specific and independent probability distribution  $\mathcal{X}_i$ . To find the probability  $\mathcal{P}(X_j, j \neq i < X_i)$ , that means for each value of  $x_i$  we need the probability that all other variables are less than that value:

$$\text{if } X_i = l, X_j, j \neq i < l \quad (51)$$

So that could be calculated by the sum:

$$\mathcal{P}(X_j, j \neq i < X_i) = \sum_l \mathcal{P}(X_i = l) \times \mathcal{P}(X_j, j \neq i < l) \quad (52)$$

For continuous random variable distribution, the equation (52) could be expressed by:

$$\mathcal{P}(X_j, j \neq i < X_i) = \int_{-\infty}^{+\infty} PDF_{X_i}(l) \times \prod_{j=1, j \neq i}^n CDF_{X_j}(l) dl \quad (53)$$

#### ACKNOWLEDGMENT

The authors would like to thank the SPATIAL MODULATION project funded by the French National Research Agency (ANR)

#### REFERENCES

- [1] L. Atzori, A. Iera, and G. Morabito, 'The internet of things: A survey', *Computer networks*, vol. 54, no. 15, pp. 2787–2805, 2010.
- [2] M. Di Renzo, H. Haas, A. Ghayeb, S. Sugiura, and L. Hanzo, 'Spatial modulation for generalized mimo: Challenges, opportunities, and implementation', *Proceedings of the IEEE*, vol. 102, no. 1, pp. 56–103, 2014.
- [3] S. Ganesan, R. Mesleh, H. Ho, C. W. Ahn, and S. Yun, 'On the performance of spatial modulation ofdm', in *2006 Fortieth Asilomar Conference on Signals, Systems and Computers*, IEEE, 2006, pp. 1825–1829.
- [4] A. Stavridis, S. Sinanovic, M. Di Renzo, H. Haas, and P. Grant, 'An energy saving base station employing spatial modulation', in *2012 IEEE 17th International Workshop on Computer Aided Modeling and Design of Communication Links and Networks (CAMAD)*, IEEE, 2012, pp. 231–235.
- [5] J. Jeganathan, A. Ghayeb, and L. Szczecinski, 'Spatial modulation: Optimal detection and performance analysis', *IEEE Communications Letters*, vol. 12, no. 8, pp. 545–547, 2008.
- [6] R. Mesleh, H. Haas, C. W. Ahn, and S. Yun, 'Spatial modulation—a new low complexity spectral efficiency enhancing technique', in *Communications and Networking in China, 2006. ChinaCom'06. First International Conference on*, IEEE, 2006, pp. 1–5.
- [7] Y. A. Chau and S.-H. Yu, 'Space modulation on wireless fading channels', in *Vehicular Technology Conference, 2001. VTC 2001 Fall. IEEE VTS 54th*, IEEE, vol. 3, 2001, pp. 1668–1671.
- [8] H. Haas, E. Costa, and E. Schulz, 'Increasing spectral efficiency by data multiplexing using antenna arrays', in *Personal, Indoor and Mobile Radio Communications, 2002. The 13th IEEE International Symposium on*, IEEE, vol. 2, 2002, pp. 610–613.
- [9] R. Y. Mesleh, H. Haas, S. Sinanovic, C. W. Ahn, and S. Yun, 'Spatial modulation', *IEEE Transactions on Vehicular Technology*, vol. 57, no. 4, pp. 2228–2241, 2008.
- [10] J. Jeganathan, A. Ghayeb, L. Szczecinski, and A. Ceron, 'Space shift keying modulation for mimo channels', *IEEE Transactions on Wireless Communications*, vol. 8, no. 7, pp. 3692–3703, 2009.

- [11] A. Younis, N. Serafimovski, R. Mesleh, and H. Haas, 'Generalised spatial modulation', in *2010 Conference Record of the Forty Fourth Asilomar Conference on Signals, Systems and Computers*, IEEE, 2010, pp. 1498–1502.
- [12] J. Jeganathan, A. Ghrayeb, and L. Szczecinski, 'Generalized space shift keying modulation for mimo channels', in *Personal, Indoor and Mobile Radio Communications, 2008. PIMRC 2008. IEEE 19th International Symposium on*, IEEE, 2008, pp. 1–5.
- [13] R. Y. Chang, S.-J. Lin, and W.-H. Chung, 'New space shift keying modulation with hamming code-aided constellation design', *IEEE Wireless Communications Letters*, vol. 1, no. 1, pp. 2–5, 2012.
- [14] Z. Bouida, H. El-Sallabi, A. Ghrayeb, and K. A. Qaraqe, 'Enhanced space-shift keying (ssk) with reconfigurable antennas', in *Communications (ICC), 2015 IEEE International Conference on*, IEEE, 2015, pp. 2393–2398.
- [15] C.-C. Cheng, H. Sari, S. Sezginer, and Y. T. Su, 'Enhanced spatial modulation with multiple signal constellations', *IEEE Transactions on Communications*, vol. 63, no. 6, pp. 2237–2248, 2015.
- [16] A. Mokh, M. H elard, and M. Cruss iere, 'Space shift keying modulations for low complexity internet-of-things devices', in *2017 Global Communications Conference (GLOBECOM)*, IEEE, 2017.
- [17] L.-L. Yang, 'Transmitter preprocessing aided spatial modulation for multiple-input multiple-output systems', in *Vehicular Technology Conference (VTC Spring), 2011 IEEE 73rd*, IEEE, 2011, pp. 1–5.
- [18] D.-T. Phan-Huy and M. H elard, 'Receive antenna shift keying for time reversal wireless communications', in *2012 IEEE International Conference on Communications (ICC)*, IEEE, 2012, pp. 4852–4856.
- [19] Y. Kokar, J.-C. Prevo et, and M. Helard, 'Receive antenna shift keying modulation testbed for wireless communications systems', in *Globecom Workshops (GC Wkshps), 2016 IEEE*, IEEE, 2016, pp. 1–6.
- [20] A. Mokh, Y. Kokar, M. H elard, and M. Cruss iere, 'Time reversal receive antenna shift keying on mimo los channel', in *2017 International Conference on Sensors, Networks, Smart and Emerging Technologies (SENSET)*, IEEE, 2017.
- [21] A. Stavridis, S. Sinanovic, M. Di Renzo, and H. Haas, 'Transmit precoding for receive spatial modulation using imperfect channel knowledge', in *Vehicular Technology Conference (VTC Spring), 2012 IEEE 75th*, IEEE, 2012, pp. 1–5.
- [22] R. Zhang, L.-L. Yang, and L. Hanzo, 'Generalised precoding aided spatial modulation', *IEEE Transactions on Wireless Communications*, vol. 12, no. 11, pp. 5434–5443, 2013.
- [23] A. Stavridis, M. Di Renzo, and H. Haas, 'Performance analysis of multistream receive spatial modulation in the mimo broadcast channel', *IEEE Transactions on Wireless Communications*, vol. 15, no. 3, pp. 1808–1820, 2016.
- [24] C. Masouros and L. Hanzo, 'Dual-layered mimo transmission for increased bandwidth efficiency', *IEEE Transactions on Vehicular Technology*, vol. 65, no. 5, pp. 3139–3149, 2016.
- [25] A. Mokh, M. H elard, and M. Cruss iere, 'Extended receive antenna shift keying', in *2017 IEEE International Conference on Telecommunication (ICT)*, IEEE, 2017.
- [26] A. Mokh, M. Cruss iere, and M. H elard, 'Performance analysis of the maximum ratio transmission preprocessing for extended receive antenna shift keying', in *2017 International Symposium on Wireless Personal Multimedia Communications (WPMC)*, IEEE, 2017.
- [27] K. Ishibashi and S. Sugiura, 'Effects of antenna switching on band-limited spatial modulation', *IEEE Wireless Communications Letters*, vol. 3, no. 4, pp. 345–348, 2014.